Temperature behaviour of photoluminescence and electron-beam-induced current recombination behaviour of extended defects in solar grade silicon

2002 J. Phys.: Condens. Matter 14 13169

(http://iopscience.iop.org/0953-8984/14/48/365)

INSTITUTE OF PHYSICS PUBLISHING JOURNAL OF PHYSICS: CONDENSED MATTER

J. Phys.: Condens. Matter **14** (2002) 13169–13177 PII: S0953-8984(02)54027-3

Temperature behaviour of photoluminescence and electron-beam-induced current recombination behaviour of extended defects in solar grade silicon

Tz Arguirov[1,3], W Seifert[1,2], M Kittler[1,2] and J Reif[1,3]

[1] Joint Lab IHP/BTU, Universitätsplatz 3-4, 03044 Cottbus, Germany
[2] IHP, Im Technologiepark 25, 15236 Frankfurt (Oder), Germany
[3] BTU Cottbus, Lehrstuhl Experimentalphysik II, Universitätsplatz 3-4, 03044 Cottbus, Germany

Received 27 September 2002
Published 22 November 2002
Online at stacks.iop.org/JPhysCM/14/13169

Abstract

The temperature dependence of D-band and band-to-band (BB) luminescence was measured in EFG samples between 80 K and room temperature for defects/dislocations presenting different amounts of contamination. The contamination density was estimated from the temperature behaviour of the electron-beam-induced current contrast, ranging between about 10^4 and 10^6 impurities cm^{-1} dislocation length. The D1 line became already visible at room temperature but its intensity was found to exhibit a maximum at about 150 K. D2, D3 and D4 start to show up at about 250, 190 and 170 K, respectively, and increase their intensities upon lowering temperature. At room temperature the width of the D1 line is broad and becomes narrower upon lowering the temperature. D2 shows the opposite behaviour. The intensities of D1 and D2 were observed to show strong variations across the sample, whereas this was not observed for the pair D4/D3. In particular, the origin of the lines D1 and D2 is still far from being understood. Two more lines at 1.040 and 0.987 eV were found in regions where the BB recombination is strong. They appear without any defect contribution and are explained as phonon replicas of the band edge luminescence.

1. Introduction

Since the discovery of D-band luminescence on dislocations in plastically deformed Cz silicon by Drozdov *et al* in 1976 [1] a lot of effort has been made to understand the origin of the dislocation activity. D-band luminescence could be found in different silicon samples containing dislocations such as, for example, plastically deformed silicon [1–3], SiGe epilayers on Si [4–6], or multicrystalline silicon (mc-Si) [7, 8]. It has been suggested that the D lines could be classified in pairs D4/D3 and D2/D1, because of their similar temperature behaviour and reaction to uniaxial stress [8]. It is believed that the D4 line is caused by radiative transitions between the shallow one-dimensional bands, formed by the dislocation strain field and that

D3 is a phonon replica of D4 (e.g. [10]). The nature of D1 and D2 is still unclear. Higgs *et al* [11] correlated the appearance of D1 and D2 with transitions on point defects in the vicinity of dislocations, where metal contamination and self-interstitials play a key role in the process. Other studies by Pizzini *et al* [12] showed that oxygen precipitates strongly enhance D1 and D2 luminescence, leaving D3 and D4 almost unaffected. However, there are still many open questions regarding the D-band luminescence in Si.

The rapid development of photovoltaics during the last decades increased interest in dislocation related defects in Si, as it was found that dislocations are the main cause for 'defect' sites in solar grade materials. Studies on mc-Si [13, 14] showed that regions with enhanced D-band luminescence exhibit high recombination activity too, resulting in a reduced minority-carrier diffusion length and strong quenching of band edge luminescence. Consequently, photoluminescence (PL) exhibits a strong potential for non-destructive monitoring of silicon materials regarding defects (e.g. [7, 8, 13–15]).

Furthermore, the D1 band luminescence is also of interest for microelectronics. Work is being done to increase the dislocation-related optical emission at 1.55 μm for developing silicon based light emitting devices to be used for optical interconnection between transistors in integrated circuits (e.g. [4] and the paper of E A Steinman at this conference).

The recombination properties of extended crystal defects in Si are strongly affected by impurities decorating the particular defects (e.g. [6]). That means the recombination activity cannot be attributed simply as an intrinsic defect property. Temperature-dependent investigations of the recombination activity of dislocations, using the electron-beam-induced current (EBIC) technique, clearly proved the role of defect contamination (e.g. [6]). Both the magnitude of the EBIC contrast and its temperature dependence $c(T)$ have been found to depend on the density of contamination at the crystal defects. Clean dislocations exhibit only very weak activity (type II), with a maximum at about 50 K and untraceable activity at room temperature. Weak contamination leads to an increase of the low temperature activity, still leaving the room temperature activity below the detection limit (type 2). With further increase of the contamination the type of temperature dependence changes and defect activity is detected at room temperature, too (mixed-type and type 1). A similar influence of contamination was observed for defects formed by oxygen precipitation in Cz-Si. A model that combines the effects of shallow intrinsic defect levels and deep contamination induced centres has recently been published (see [17]). The model assumes that shallow one-dimensional dislocation bands, induced by the dislocation strain field, and deep electronic levels, caused by segregated impurity atoms at the dislocations, can exchange electrons and holes. As a consequence, the recombination of carriers captured at the dislocation bands can be drastically enhanced by the presence of even small concentrations of impurity atoms at the dislocation core. The model delivers the following concentration of impurities for the various types of behaviour: type II—clean, type 2—about 10^4–10^5 impurities cm^{-1} dislocation length, type 1—few 10^6 impurities cm^{-1} or more (for the mixed-type behaviour the number of impurities is between types 1 and 2).

It was found that D-band luminescence becomes detectable only for dislocations of type 1, 2 and mixed-type EBIC behaviour and results in quenching of band-to-band (BB) luminescence (e.g. [6, 11]). Here, we deal with investigations of EFG-Si, a strongly inhomogeneous material containing a variety of extended defects and impurities.

2. Experimental details

We investigated mc-Si ribbons produced by the EFG process (e.g. [13]). For the EBIC measurements Schottky contacts were prepared by evaporation of Al. EBIC investigations

between 80 K and room temperature were done before the PL measurements, in order to estimate the amount of contamination at the extended defects/dislocations.

For the PL measurements, the surface contact was removed by etching. The surface left after the etching procedure was sufficiently clean from non-radiative surface centres, allowing us to detect BB and 'defect' luminescence even at room temperature. Green light 514.5 nm from an argon-ion laser with 300 mW power was used as the excitation source. The probe beam, directed normally to the sample surface, was focused to a spot of 100 μm. The spot size was controlled by scanning a silicon sample, partially covered by a stripe of deposited aluminium. The reflected light intensity profile around the stripe edge was fitted with a convolution of a Gaussian and a step function. The size of the spot was determined from the best fitting width of the Gauss curve.

Back-emitted luminescent light was collected by a parabolic mirror and analysed by a spectrometer equipped with a 300 grooves mm^{-1} grating monochromator and liquid-nitrogen-cooled Ge detector. We estimated the local temperature increment due to the focused laser beam according to the model, described in [18]. In the conditions of our experiment we found that the temperature difference due to local heating does not exceed 5 K, so we did not consider it further.

3. Results

Figure 1 compares PL (a, c) and EBIC (b, d) results obtained at room temperature (a, b) and at 80 K (c, d), respectively. Regions with high defect density exhibit strong recombination activity and appear as dark areas in EBIC. A PL scan was carried out along the growth direction of the EFG foil, i.e. along the vertical direction with respect to figure 1. The measurements were done along a line of points, 100 μm apart. At each point a PL spectrum was recorded in the wavelength interval 1000–1700 nm; two single spectra are shown in figure 2. The images (figures 1(a) and (c)) present in grey scale the luminescent light intensity versus the wavelength and the position on the sample where it was measured. Such scans were made for 12 different temperatures in the interval 80–300 K.

Both PL and EBIC detect the existence of areas with a high density of active defects. The sites exhibiting EBIC contrast at room temperature show a reduced BB luminescence and an enhanced defect (D1) luminescence in the PL scan. At 80 K their EBIC activity becomes higher and some other areas, inactive at room temperature, appear with detectable contrast. Such temperature behaviour (mixed type and type 2) is characteristic for defects with a density of contamination ranging between 10^4 and 10^6 impurity atoms cm^{-1} dislocation length [14, 17]. The PL scan taken at 80 K shows a remarkable reduction of BB and enhanced defect-band luminescence at the EBIC active sites. The four (D1–D4) dislocation related luminescence lines can be found in the spectra.

The EFG material studied is characterized by a strongly inhomogeneous distribution of extended defects and impurities (oxygen, carbon, metals). This is clearly reflected by figure 1 representing the inhomogeneities in EBIC and PL. In the following, we deal with the spatial distribution of the D lines, with the temperature dependence of the D line intensity and D line peak position, with details of the temperature dependence of the width of the D1 and D2 lines, and also with the appearance of characteristic lines below the energy of the BB luminescence. It should be noted that many data shown below represent extreme features that were observed during our measurements in specific regions. A detailed analysis of these regions regarding structural and chemical peculiarities and a comparison with the less disturbed regions of the EFG material has not yet been finished and will be reported later.

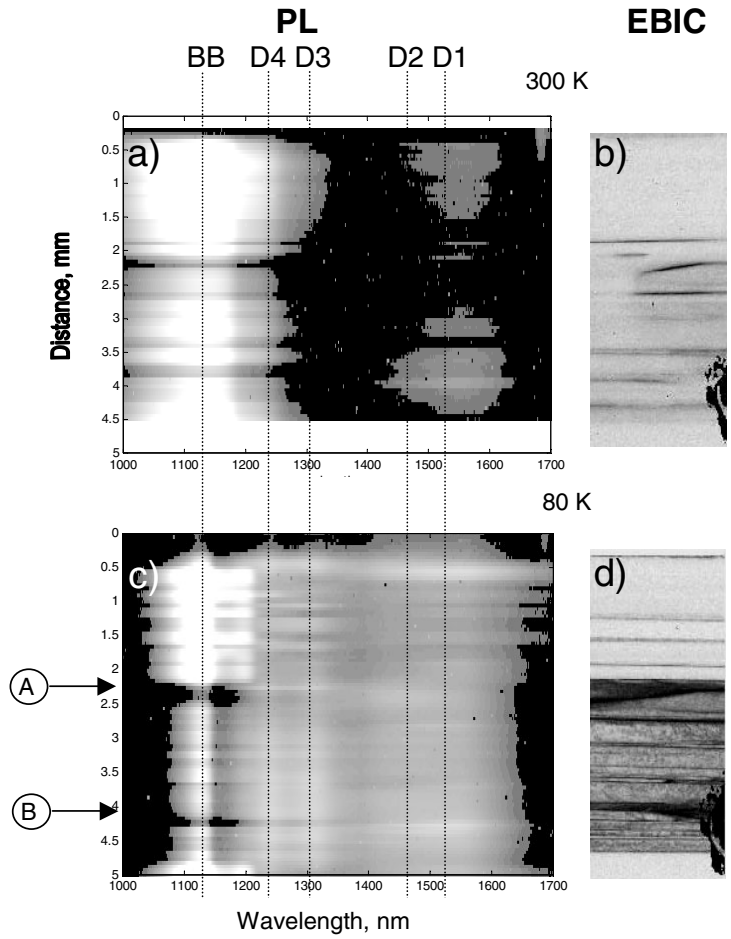

Figure 1. Comparison between PL scans and EBIC micrographs at 300 and 80 K. Luminescence spectra were taken sequentially along a vertical line over the sample. The intensity of luminescent light is given in grey scale with regard to its wavelength and the position on the sample. D lines (D1, D2, D3 and D4) and BB luminescence are marked by broken lines. Single spectra from positions A and B are presented in figure 2.

3.1. Spatial distribution of D lines

At first we report on PL spectra measured in two peculiar regions, denoted A and B and marked in figure 1(c). At room temperature the BB luminescence on both places is strongly reduced there. A significant D1 luminescence can be observed only in region B, but it is missing in region A. This difference can also be found at 80 K. Figures 2(a) and (b) compare spectra taken at 80 K at positions A and B, respectively. The spectra were numerically deconvoluted into 4 or 5 Gaussian peaks. The spectrum at position A shows a very weak D1 line. The D1 peak area is about one order of magnitude smaller than that of D2. In comparison, the D1 line at position B is significantly stronger and its amplitude is comparable with the D2 amplitude. D3 and D4 show almost the same intensity/peak area at both positions. It is also worth noting that the BB luminescence is stronger, when the sum of D1, D2, D3 and D4 line intensities becomes smaller.

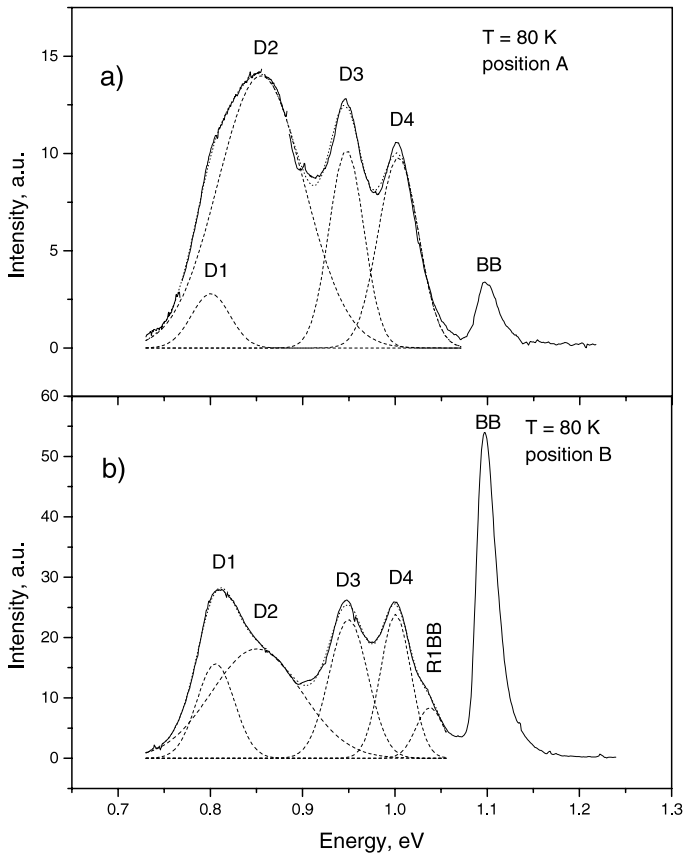

Figure 2. PL spectra taken at positions A and B (see figure 1). The broken curves are Gaussians, obtained by numerical deconvolution of the spectra. The intensity and width of D3 and D4 remain similar, whereas the D1 and D2 peak areas vary strongly. At position A the peak area of D1 is one order of magnitude smaller than D2. D2 always appears broader than the other D lines.

Generally, strong spatial variations of peak amplitudes/intensities occur for D1 and D2 along the entire scan, whereas D3 and D4 maintain their relation almost constant. It is also found that D1, D3 and D4 exhibit nearly the same peak width and that D2 is about two times broader (see below). The fact that there are strong variations observed for the intensities of D1 and D2 along the sample, whereas such variations cannot be found for D3 and D4, indicates that the recombination processes of D4/D3 differ from those of D2/D1. It confirms the view that D4 and D3 occur as a couple, whereby D3 is formed as a phonon replica of D4. However, it is hard to believe that D1 and D2 also represent a pair, although the energy difference D2 − D1 was found to exhibit about $\Delta E = 50$ meV, i.e. the same value as the difference D4 − D3 (see table 1). It has been suggested by Higgs *et al* [11] that D1/D2 originate from point defects trapped in the vicinity of dislocations.

3.2. Temperature dependence of D-line intensity

Figure 3 depicts the temperature dependence of the intensity of the D lines measured in a defect region located between positions A and B (compare figure 1). The intensity of radiative recombination at the dislocations was observed to increase upon lowering temperature. This is

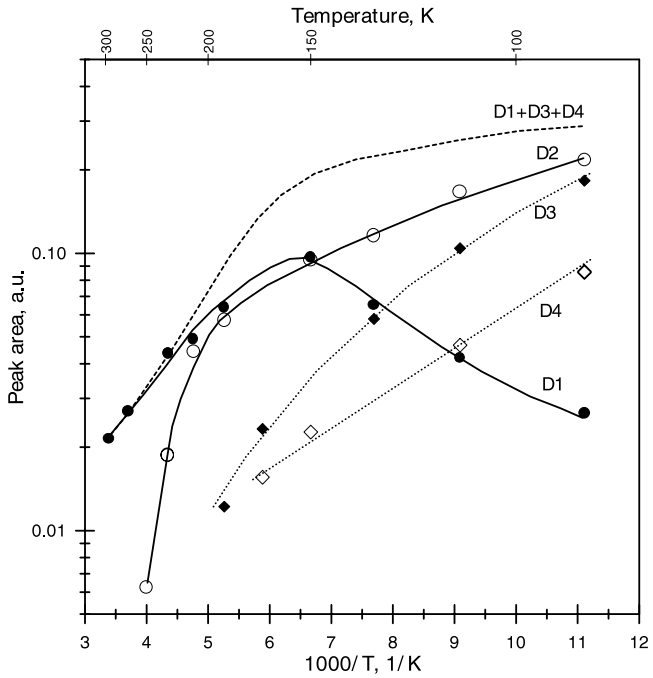

Figure 3. Temperature dependence of peak areas/intensities. D2, D3 and D4 increase upon lowering temperature. At high temperatures D1 follows the behaviour of D2 but after the appearance of D3 and D4 it starts to decrease upon lowering the temperature. For comparison, the sum of D1, D3 and D4 is shown as a broken curve.

Table 1. Mean position of the peaks observed in photoluminescent spectra. Together with the four D-band lines two more lines were observed, R1BB and R2BB.

	Peak position (eV)		
	Single crystal [1]	mc-Si [8]	This study
D1	0.812	0.80	0.80
D2	0.875	0.83–0.89	0.85
D3	0.934	0.95	0.95
D4	1.000	1.00	1.00
R1BB			1.040
R2BB			0.987

in agreement with the observations made by other authors as well (e.g. [8], [20]). D1 is already found as a broad defect band at room temperature and D2 becomes detectable at about 250 K. D3 appears at about 190 K and D4 at 170 K. Except for D1, the intensities/peak areas of the other lines follow an almost exponential enhancement upon lowering temperature. At about 150 K, immediately after the appearance of D3 and D4, the D1 line changes its behaviour and starts to diminish upon further decrease of the temperature. According to our knowledge such a behaviour of D1—exhibiting a maximum at about 150 K—has not been yet described in the literature. It is also interesting to note that the sum of the peak areas of D1, D3 and D4 lines results in a curve which runs nearly parallel to the temperature behaviour of D2.

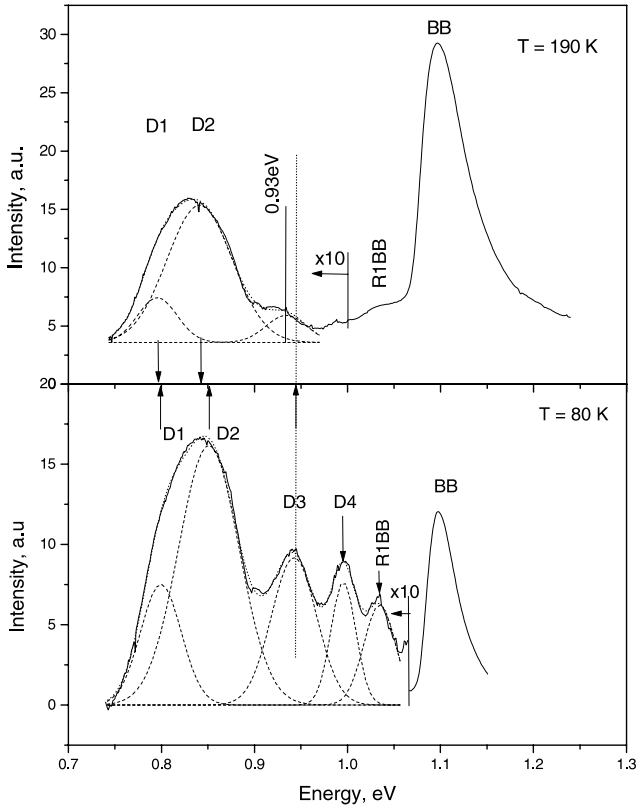

Figure 4. The peak at 0.93 eV deconvoluted from the spectrum taken at 190 K (a) is identified as D3. Upon decreasing the temperature it moves up to the well-known position of D3, see the spectrum at 80 K (b).

3.3. D-line peak positions and their temperature dependence

PL studies on mc-Si showed that the maximum of the D lines are slightly shifted compared to those obtained for plastically deformed Cz silicon (e.g. [13]). Differences of about 15 meV were found for D1, D2 and D3, although D4 stayed almost unaffected. The results of the numerical deconvolution of our 80 K spectra are given in table 1, together with the data reported in [1, 8].

Fukatsu *et al* [19] found that the positions of D1 and D2 exhibit a temperature shift which is opposed to D3/D4. Increasing the temperature, the D3/D4 peaks move to higher energies, while D1 and D2 were observed to move downwards to lower energies together with the BB line. The same trend for D1 and D2 was confirmed by our measurements. However, D3 does not show the expected trend. It appears at 80 K as a well resolved peak (figure 4(b)) with a maximum at 0.95 eV. At higher temperatures it shifts to lower energies together with D1 and D2. The highest temperature, where D3 can be detected as a shoulder next to D2, is about 190 K. The deconvolution gives for D3 an energy of about 0.93 eV (figure 4(a)).

3.4. Temperature dependence of the width of D1 and D2

Another interesting feature regarding D1 and D2 is illustrated in figure 5. It represents the evolution of the peak width of D1 and D2 with temperature, as measured at the sample region

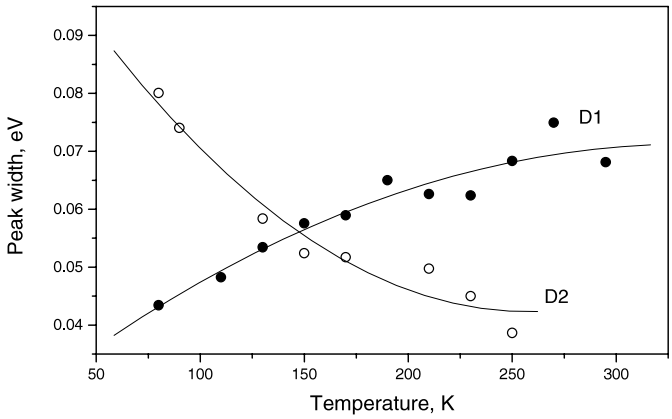

Figure 5. Temperature dependence of the peak width of D1 and D2. D1 becomes narrower and D2 broader upon decreasing temperature. The full curves are guides for the eyes only.

located between positions A and B (compare figure 1). As previously noted, only one broad D1 peak can be observed at room temperature. D2 appears as a narrow band next to D1 at about 250 K. D2 becomes broader and D1 narrower when the temperature is lowered further. At about 150 K both lines show the same width. D1 and D2 change their width by a factor of about two within the entire temperature range. A similar behaviour for D1 has been reported in luminescence from diodes on plastically deformed Cz-Si [10].

3.5. Characteristic lines below the energy of the band-to-band luminescence

Two more features, R1BB at 1.04 eV and R2BB at 0.987 eV, were found in the PL spectra (see table 1). R1BB can be seen in figures 2(b) and 4(b). R2BB can only be detected in regions where BB recombination is very strong. The maxima of the peaks are shifted by (phonon) energies of about 60 meV for R1BB and 120 meV for R2BB, respectively, relative to the peak of BB luminescence (1.1 eV). An experiment under identical conditions on float-zone silicon showed the presence of these lines, too. Consequently, they appear without any defect contribution and presence of D-band radiation. The lines R1BB and R2BB are believed to be phonon replicas of the BB luminescence.

4. Conclusions

Many of our observations made on EFG Si are in agreement with data on D-band luminescence found in other materials. However, some features have not been described in the literature before. An improved insight into the origin of D lines cannot be deduced from our data presented here. In particular, the formation of the D1 and D2 lines is still mysterious. Nevertheless, we learned that further experiments on well-defined Si samples containing dislocations formed by different methods and being contaminated with different species will be needed, to allow separation of general and very specific features of D-band luminescence. It is believed that data measured at samples containing well-defined 'model defects' would help in making progress on the origin of D-band lines and to develop a joint model which allows us to describe both the PL and EBIC observations.

Acknowledgments

The authors would like to thank Dr S Ostapenko for helpful suggestions about the design and optimization of our PL apparatus, for his advice and discussion related to Si-based luminescence and for providing the EFG samples.

References

[1] Drozdov N A, Patrin A A and Tkachev V D 1976 *JETP Lett.* **23** 36
[2] Sekiguchi T and Sumino K 1996 *J. Appl. Phys.* **79** 3253
[3] Kveder V V, Steinman E A and Grimmeiss H G 1996 *Solid State Phenom.* **47–48** 419
[4] Kveder VV, Steinman E A and Grimmeiss H G 1995 *J. Appl. Phys.* **78** 446
[5] Higgs V, Lightowlers E C, Tajbakhsh S and Wright P J 1992 *Appl. Phys. Lett.* **61** 1087
[6] Kittler M, Ulhaq-Bouillet C and Higgs V 1995 *J. Appl. Phys.* **78** 4573
[7] Tarasov I, Ostapenko S, Hässler C and Reisner E U 2000 *Mater. Sci. Eng.* B **71** 51
[8] Ostapenko S, Tarasov I, Kalejs J P, Hässler C and Reisner E U 2002 *Semicond. Sci. Technol.* **15** 840
[9] Sauer R, Weber J, Stolz J, Weber E R, Küsters K H and Alexander H 1985 *Appl. Phys.* A **36** 1
[10] Kveder V V, Steinman E A, Shevchenko S A and Grimmeiss H G 1995 *Phys. Rev.* B **51** 10520
[11] Higgs V, Chin F, Wang X, Mosalski J and Beanland R 2000 *J. Phys.: Condens. Matter* **12** 10105
[12] Pizzini S, Guzzi M, Grilli E and Borionetti G 2000 *J. Phys.: Condens. Matter* **12** 10131
[13] Koshka Y, Ostapenko S, Tarasov I, McHugo S and Kalejs J P 1999 *Appl. Phys. Lett.* **74** 1555
[14] Kittler M, Seifert W, Arguirov T, Tarasov I and Ostapenko S 2002 *Sol. Energy Mater. Sol. Cells* **72** 465
[15] Higgs V, Chin F and Wang X 1998 *Solid State Phenom.* **63–64** 421
[16] Kittler M and Seifert W 1995 *Phys. Status Solidi* a **150** 463
[17] Kveder V, Kittler M and Schröter W 2001 *Phys. Rev.* B **63** 115208
[18] Moody J E and Hendel R H 1982 *J. Appl. Phys.* **53** 4364
[19] Fukatsu S, Mera Y, Inoue Y, Meada K, Akiyama H and Sakaki H 1996 *Appl. Phys. Lett.* **68** 1889
[20] Steinman E A, Kveder V V, Vodovin V I and Grimmeiss H G 1999 *Solid State Phenom.* **69–70** 23